

ICMPC_2018

Dynamic FEA analysis and optimization of a robotic arm for CT image guided procedures

Ayan Roy^a, Taniya Ghosh^b, Ruby Mishra^c, Shah Shubham Kamlesh^d^aSME,KIIT University, Patia, Bhubaneswar, 751024, India^bSME,KIIT University, Patia, Bhubaneswar, 751024, India

Abstract

Cancer and tumour detection is a very essential diagnostic process. The procedure of biopsy with the help of robotic technologies to collect tissue sample is an expensive ordeal and available only in very high end hospitals. An effort was made to develop a robotic arm that will be cost effective in the procedure of biopsy. Prime objective of this research is to determine the structural accuracy of the robotic arm in long run. The virtual model of the robotic arm was designed in Solid Works 2016. Different views of the design are shown in this paper. An experimental model of the robotic arm was manufactured to check deviation in reaching a user defined target point. The design was subjected to finite element analysis in ANSYS 15.0. Study of the stress and strain analysis is done during its dynamic behaviour. Having attained the results of the analysis, further modifications are made in the model to obtain optimized deformation, stress and strain results. A net reduction in the maximum total deformation by 91.499% is achieved by making some required alteration. With these modifications, the accuracy of this robotic arm will be maintained for a longer period of time and provide better application in the medical field.

© 2018 Elsevier Ltd. All rights reserved.

Selection and/or Peer-review under responsibility of Materials Processing and characterization.

Keywords: SolidWorks 2016; ANSYS 15.0; 5-axes Robotic Arm Model; Dynamic Analysis

1. Introduction

Biopsy refers to the extraction of tissue samples for determination of presence of a disease. In needle biopsy, a long fine needle is inserted in the suspected area to collect tissue sample. In most common practices, the concerned area is tracked down by CT scan and then, a needle is inserted by the doctor. Currently the accuracy of insertion of

* Corresponding author. Tel.: +91-9475914958

E-mail address: 1502520@kiit.ac.in

2214-7853© 2018 Elsevier Ltd. All rights reserved.

Selection and/or Peer-review under responsibility of Materials Processing and characterization.

needle is dependent on eye ball method. To optimize the accuracy of biopsy, robotic technologies are put into application. However, these technologies are a lot expensive and available only in a few high grade hospitals across the world. Thus, these are not easily accessible to common people. To curb these problems, a robotic arm is designed. The basic principle of the robotic arm is to take the coordinates, determined by imaging tests, as input in the Arduino, which in turn, directs the needle automatically to the target location.

In simple words, Dynamic Analysis is the study of any structure which is subjected to dynamic loading. Dynamic load is any load that varies in magnitude, sense and direction. For complex structure, finite element analysis is carried out to study the dynamic behaviour of the structure. It is thus, important to perform the dynamic analysis of the robotic arm. The robotic arm is hence, subjected to finite element analysis in ANSYS 15.0 to determine the effects of the dynamic forces acting on it, along with the effect of its self-weight.

In this paper, we have made an attempt to study the Von-Mises stress and strain acting on each link and joint of the robotic arm during its dynamic behaviour and optimize the obtained results. The prototype would be expected to be durable and efficient in the long run in order to make up for its price. Thus, the alternative for the stress reduction in some of the stress-prone parts have been proposed by making certain adjustment in the model.

1.1. Literature Review

In the paper of Nitin Kumar KC et. al., a virtual CAD model of a human femur bone was designed with required dimensions and subjected to stress analysis, during activities like jumping, standing, walking and running, in ANSYS. In all the above cases, the knee joint was treated as the loading end whereas the femoral head was treated as fixed end and the effect of muscle on femoral bone was neglected. Except for standing (where the moment of the knee joint was considered 0), moment was considered to be 10000N-mm. After carrying out stress analysis, it was observed that the stress developed during running was below the safety stress level and optimum in the other cases.^[1]

In the paper of Ju Yi et. al., traditional methods used in pipe cutting reduces the surface quality of the pipe. In order to overcome this problem, CAD model of a virtual bearing choke model and a steel pipe was developed and subjected to finite element analysis in ANSYS. The results obtained confirmed that the maximum deformation in the bearing choke was within the allowable range and the most stress variation occurred in the contact area between the tool and steel pipe. The results of feed rate were also within the allowable range thereby, assuring the model's compatibility to meet the requirements.^[2]

In the paper of Chen Yanhong et. al., an YJ3128-type dump truck's sub frame was subjected to stress analysis in ANSYS. Experimentally, fatigue cracks were observed in the sub-frame after the truck is worked with in rough conditions for 3-5 months. Since the roads travelled by the trucks were uneven, the lifting height of the frame was set to 20mm and 50mm and analysis of the beam was conducted. Having performed the analysis it was determined that the maximum stress concentration was at the right side of the square beams and the turning point of the left stringer, which contributed as the main reason for the failure of the frame. To overcome this problem, a beam was added in front of the sub-frame to increase its torsional stiffness.^[3]

In the paper of Martin Močilan et. al., the dynamics of fluid in a tank was studied with an approach to overcome sloshing effect of the fluid on the container. For this, CFD modelling analysis was undertaken. For further optimization of fuel tank, different other conditions of baffles can be taken under consideration which were neglected here.^[4]

In the paper of Praveen Silori et. al., fatigue analysis of traction gear assembly was carried out for different materials. Analytically, it was found that AISI 4041 Steel alloys have got good bending resistance characteristics as compared to Ti6242S alloys. However, Ti6342S alloys are preferred over AISI 4041 for its better service life and fail safe design.^[5]

2. Methodology

The CAD model of the robotic arm was first delineated in SolidWorks 2016. It was then subjected to finite element analysis in ANSYS 15.0. Having obtained the stress and deformation results, it was necessary to make some modifications in the model to reduce the maximum stress induced and the maximum extent of deformation in link 2.

2.1. Designing

The designed motors are the joints whereas all the Aluminium parts (couples and bars) are the links. The joints and links are numbered sequentially on the basis of their respective remoteness from the fixed Cast iron base.

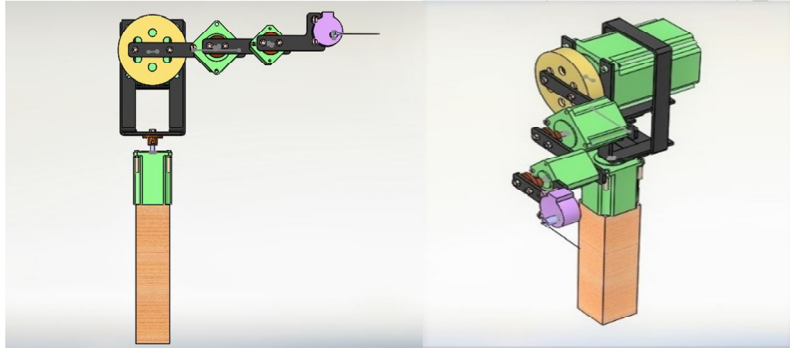


Figure 1: (a) Front view of the robotic arm; (b) Isometric view of the robotic arm

Joint 1 is the stepper motor connected to the base. Joint 1 provides rotary motion to link 1, which is connected with joint 2, as shown in the figure of the model. Joint 2 provides rotary motion to link 2, in a direction perpendicular to the plane of motion of link 1. Joint 3 is bolted with link 2 and therefore, rotates along with it. Joint 3 provides rotary motion to link 3 in the same plane as the motion of link 2. Joint 4 is attached to link 3 thus, following its path of rotation. In the very similar plane of motion, link 4 is rotated by joint 4. Link 4 is joined to joint 5, which provides rotary motion to the needle, which is link 5, in the identical plane.

The black bars and the yellow and brown couplings in figure 1(a), act as the links of the robotic arm. The four green and one purple stepper motor, shown clearly in figure 1(b), act as the joints of the robotic arm. From the figures above, it can be perceived that the plane of motion of joint 2,3,4,5 are similar and perpendicular to the plane of motion of joint 1.

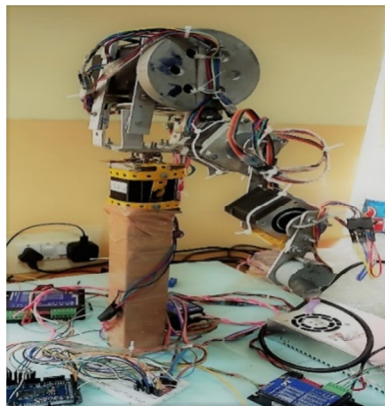


Figure 2: Working Model

An actual working model of the robotic arm is designed to verify its motion and accuracy. It is portrayed in figure 2. The first stepper motor is fixed to the cast iron base. The other stepper motors and the aluminium bars being built-in similarly to that of the model designed in SolidWorks 2016.

2.2. Initial results

The predesigned SolidWorks model of the robotic arm is subjected to finite element analysis in ANSYS 15.0. Prior to that, materials of each part of the model are specified, as shown in table 1:

Table 1. Material properties		
Material	Aluminium Alloy	Stainless Steel
Parts Specified To	Couplings and Bars	Shafts, bolts and nuts
Density	2770 kg/m3	7750 kg/m3
Young's Modulus	7.1E+10 Pa	1.93E+11 Pa
Compressive Yield Strength	2.8E+8 Pa	2.07E+8 Pa
Tensile Ultimate Strength	3.1E+8 Pa	5.8E+8 Pa
Specific Heat	875 kg/JC	480 kg/JC

The motors are bought from NEMA Company and specified as per datasheet. The base is specified as cast iron. After material initialization, meshing of the model is done with following sizing mesh parameters as shown in below Table 2:

Table 2. Sizing parameters		
Parameter	Details	Parameter
Smoothing	High	Smoothing
Transition	Slow	Transition
Element Size	Default	Element Size

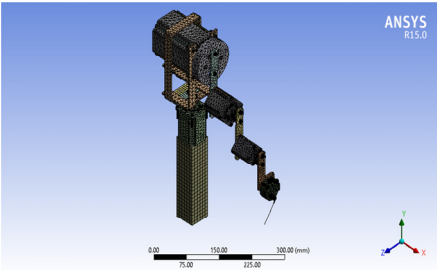


Figure 3: Meshed model

An image of the meshed model is shown in figure 3. This is followed by Von-Mises stress, strain and deformation analysis, in ANSYS 15.0, to obtain the results below.

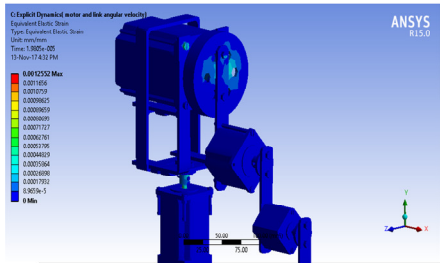


Figure 4: Equivalent Elastic strain results

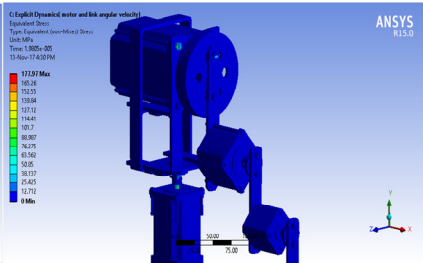


Figure 5: Equivalent stress results

The maximum strain application is observed in the couple of link 2 and the shaft of joint 1. The value so obtained of maximum equivalent elastic strain is 0.0012552 mm/mm (figure 4). The maximum stress concentration of 177.97 MPa is induced in the shaft of joint 1, which is because joint 1 bears the weight of all other parts of the robotic arm above it (figure 5).

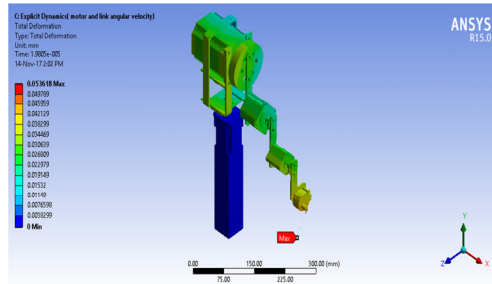


Figure 6: Total Deformation results

The maximum deformation of 0.053618mm is noticed in the link 5 (needle) of the robotic arm (figure 6). It is imperative to minimize the extent of deformation, strain and stress induced in the robotic arm to achieve maximum efficiency from it. Hence, an alternative to enhance the model is proposed ahead.

2.3. Design Modification

To optimize the above results, an extra aluminium bar in link 2 is added to the robotic arm. Figures 7 and 8 shows the isometric and side view of the enhanced model respectively.

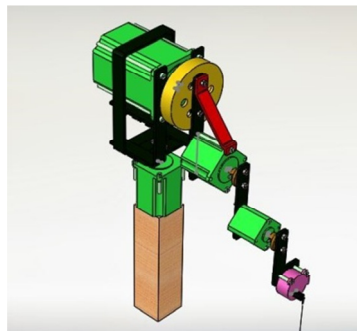


Figure 8: Isometric view (Modified Model)

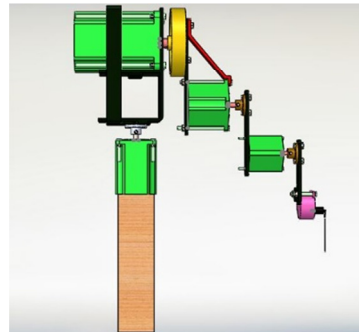


Figure 7: Side view (Modified model)

The red bar in the aforementioned figures indicates the additional bar. It makes an angle of 57.283 degree with the bolt in the upper end of joint 3. Previously, the weights of joint 3, 4 and 5 and the respective links connecting them, acted solely on the black bar of link 2. Now, the addition of the red bar, reduces the load exertion on the black bar of link 2. This leads up to decrement in the previous values of elastic strain, stress and total deformation.

3. Final Results

Having made alteration in link 2 of the robotic arm, the modified model is now subjected to meshing with same sizing parameters as the previous mode in ANSYS 15.0.

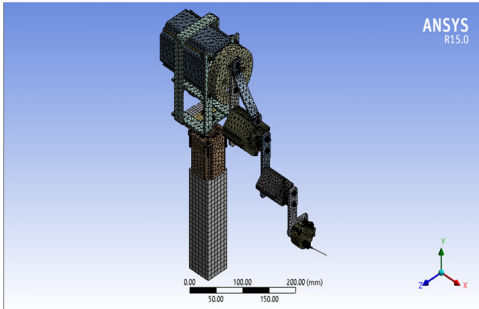


Figure 9: Meshed view (Modified model)

Von-Mises stress, strain and deformation analysis are performed in the updated model to obtain an efficient set of values as shown in above Fig 8 and Fig 9.

The addition of the extra bar in link 2 has led to a fall of elastic strain by 53.474%. The maximum strain now existing is 0.00058399 mm/mm (figure 10). The maximum stress concentration has dropped from 177.97MPa to 95.556MPa. This has significantly reduces the probability of early damage of shaft of joint 1(figure 11).

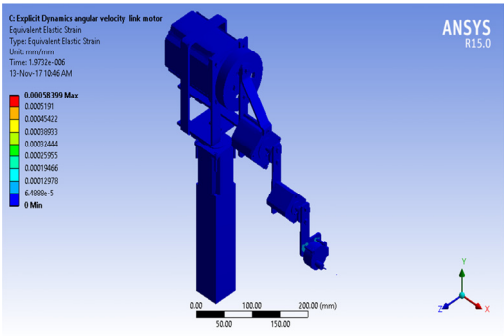


Figure 10: Elastic Strain analysis of Modified model

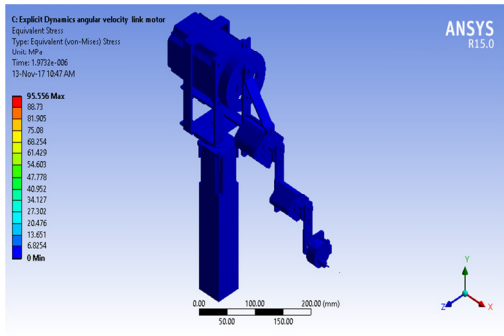


Figure 11: Stress analysis of Modified model

The total deformation has reduced by 91.499% (figure 12). The maximum deformation is now 0.0045578mm, which is a very negligible value. Thus, in all, the performed modification has proved beneficial in optimizing the stress, strain and extent deformation in the robotic arm.

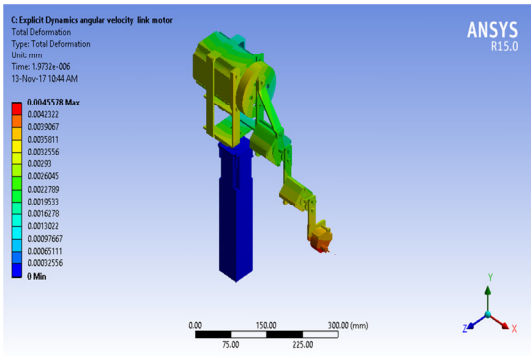


Table 3. Compared results of earlier model and modified model

Parameter	Max. Value In Previous Model	Max. Value In Modified Model
Stress	177.97 MPa	95.556 MPa
Elastic Strain	0.0012552 mm/mm	0.00058399 mm/mm
Deformation	0.053618 mm	0.0045578 mm

From the above table, it can be understood that after modifying the robotic arm, deformation during its operation has been significantly reduced by 91.499 %, stress by 46.307% and elastic strain by 53.474%. This will help the robotic arm with increased accuracy during experimental run.

4. Conclusion

This paper required the applications of SolidWorks 2016 and ANSYS 15.0 for designing the robotic arm and simulating it respectively. Having designed a virtual model of the robotic arm, a real life working model of same was manufactured with appropriate dimensions and materials. The stepper motors were signalled by Arduino. The point of extrusion of the shaft from the motor of joint 1 was the origin and the coordinates of the target location was to be determined accordingly. The accuracy of the working model was apt thus, fulfilling the purpose for which it is designed. However, the stress, strain and deformation analysis results required to be optimized so that the robotic arm could maintain its structural efficiency for longer period.

The objective of enhancing the robotic arm for its better structural accuracy has been achieved by the making the necessary change in link 2 of the model. A significant reduction of stress, elastic strain and deformation by 46.307%, 53.474% and 91.499% respectively was achieved. In the previous model, the maximum deformation was noticed in the needle. Therefore, the substantial reduction in deformation value signifies that the needle would maintain its accuracy for a long period. Also, the decline in stress concentration in the shaft of joint 1 lowers the chances of the early damage in the aforementioned shaft. Thus, the model would worth its price. This leads up to fulfilling our other objective, which was to cut down the expense and improve the practice of cancer and tumour diagnosis. Further steps will be taken to implement changes made in the virtual model into the experimental model to increase the efficiency of the robotic arm.

Acknowledgements

A humble thanks to KIIT University, Bhubaneswar, Odisha for supporting and guiding through this research and providing resources for the above research.

References

- [1] Nithin Kumar KC, Tushar Tandon, Praveen Silori, Amir Shaikh, Biomechanical stress analysis of a Human Femur bone using ANSYS, Elsevier Ltd., 2015.
- [2] Ju Yi, Yingping Qian, Zhiqiang Shang, Zhihong Yan, Yang Jiao, Structure Analysis of Planetary Pipe Cutting Machine Based on ANSYS, Elsevier Ltd., 2017.
- [3] Chen Yanhong, Zhu Feng, The Finite Element Analysis and The Optimization Design of The Yj3128-type Dump Truck's Sub-Frames Based on ANSYS, Elsevier Ltd., 2011.
- [4] Martin Močilan, Milan Žmindák, Peter Pastorek, Dynamic analysis of fuel tank, Elsevier Ltd., 2016.
- [5] Praveen Silori, Amir Shaikh, Nithin Kumar KC, Tushar Tandon, Finite Element Analysis of Traction gear using ANSYS, Elsevier Ltd., 2015.
- [6] František Klimenda, Josef Soukup, Modal analysis of thin aluminum plate, Elsevier Ltd., 2017.
- [7] Fangfang Song, Yihua Ni, Zhiqiang Tan, Optimization Design, Modeling and Dynamic Analysis for Composite Wind Turbine Blade, Elsevier Ltd., 2011.
- [8] Mahdi Kiani, Joanne Ishak, Michael W. Keller, Steven Tipton, Comparison between nonlinear FEA and notch strain analysis for modeling elastoplastic stress-strain response in crossbores, Elsevier Ltd., 2016.
- [9] Santosh S. Patil, Saravanan Karuppanan, Ivana Atanasovska, Experimental measurement of strain and stress state at the contacting helical gear pairs, Elsevier Ltd., 2016.
- [10] M.T. Schobeiri, Fluid Mechanics for Engineers, Springer, 2010.
- [11] W.S. Janna, Introduction to Fluid Mechanics, CRS Press, New York, 2009.
- [12] Tony Burton, David Sharpe, Nick Jenkins, Ervin Bossanyi. Wind Energy Handbook. John Wiley & Sons Ltd, 2001.